Study on antimony mobility in a contaminated shallow lake sediment using the diffusive gradients in thin films technique

Cheng Yao [a, b], Feifei Che [a], Xia Jiang [a, *], Zhihao Wu [a], Junyi Chen [a], Kun Wang [a]

[a] National Engineering Laboratory for Lake Pollution Control and Ecological Restoration, State Environmental Protection Key Laboratory for Lake Pollution Control, Chinese Research Academy of Environmental Sciences, Anwai, Beiyuan, Beijing, 100012, China
[b] College of Water Sciences, Beijing Normal University, Beijing, 100875, China

HIGHLIGHTS

- Environmental behavior of Sb contaminants in a shallow lake were illustrated.
- The DGT was deployed in lake to record the mobility of Sb.
- The anoxic condition in sediment was in favor of dissolution of Fe−Sb complexes.

ARTICLE INFO

ABSTRACT

Antimony is a priority environmental contaminant. Increasing attention is being paid to the behaviors and mobilities of the various Sb species in the environment. Sb speciation in the environment and the mobilities of Sb species at mining sites have been studied well, but Sb speciation and mobility in shallow lakes requires further study. Here, we studied Sb behavior in sediment of a shallow lake in the plain rivers network in Taihu Basin that suffers continual Sb inputs from textile plants. The diffusive gradients in thin films techniques (DGT) made of zirconium oxide based binding resin gel (ZrO-Chelex), agarose diffusive gel and polyvinylidene fluoride filter were deployed in water and sediment to obtain a high-resolution record in situ. The results indicated that (1) pollutants released by textile plants caused relatively high Sb(III), Sb(V) and organoantimony concentrations in the eutrophic shallow lake, (2) Sb was seldomly mobile in the oxic layer where Sb(III) was sorbed on Fe(III) oxides and gradually formed Fe−Sb complexes in the sediment, but in the anoxic environment (oxidation-reduction potential: $366 - -344$ mv) Sb(V), Fe(II) and P (V) were simultaneously released to resupply the porewater, (3) the release of Sb from solid phase is decided by the redox condition, and the rate of release is dependent on the labile Sb content of the sediment. The mobility of Sb should be given sufficient attention when the potential ecological risk of metal(loid)s in shallow lakes and wetlands sediment are evaluated.

© 2020 Elsevier Ltd. All rights reserved.

1. Introduction

Awareness of antimony (Sb) pollution from industrial plants as the hazards has increased nowadays due to adverse impact on human health if under long-term exposure. There are naturally $0.3-8.6$ mg kg^{-1} Sb in lakes sediment all around world (Pierart, A., Shahid, M. et al., 2015). Field screenings have pointed out that the growing levels of Sb in sediment in some areas. The Sb ore stibnite was extracted near the mouth of the Bellinger River in New South Wales, Australia, in 1970s. and the wetland sediment near the tailings deposits contained Sb up to 22,000 mg kg^{-1} even after the mining sites were abandoned in 1974 (Warnken, J., Ohlsson, R. et al., 2017). Textile and printing plants have caused relative high levels of Sb about 10 mg kg^{-1} in plain river-network sediments in the lower Yangtze River, China (Yao, C., Jiang, X. et al., 2019). Sb minerals are quite stable in soil and sediment. The dissolution of Sb minerals occur over a wide range of pH ($1.5 - 12$) (Zotov, A.V., Shikina, N.D. et al., 2003), but it is in favorable in slightly alkaline aqueous environment (Hu, X., He, M. et al., 2017). The solubility of Sb minerals are ordinarily followed by relative high temperature ($80 - 400$ °C) and high pressure ($0.1 - 100$ MPa) except for

* Corresponding author. National Engineering Laboratory for Lake Pollution Control and Ecological Restoration, Chinese Research Academy of Environmental Sciences, Anwai, Beiyuan, Beijing, 100012, China.
E-mail address: jiangxia@craes.org.cn (X. Jiang).

valentinite that take place under moderate environment (25 °C). Fewer studies of Sb pollution in lakes and wetlands caused by textile and printing plants than of Sb pollution in mining areas have been performed.

Studies on spatial distributions of Sb in lakes sediments around tailing deposits have indicated that Sb is less mobile than As, but it also spread out to the surrounding soil, sediment and biota (Wang, X., He, M. et al., 2011; Ungureanu, G., Santos, S. et al., 2015). Antimonate, antimonite and antimony oxyhydroxides discharged from textile and printing plants are transported through fluvial pathways and gradually accumulated in the sediment. In lake sediment, particularly in lakes near towns and factories, a large proportion of the Sb is associated with organic matter such as humic and fulvic acids (Multani, R.S., Feldmann, T. et al., 2017). Sb in sediment can be sorbed on active redox sites of Fe, Mn, Al oxides and organic matters through ligand exchange. Redox condition is a vital important factor for the mobilization that Sb would be more stable under anoxic condition due to the Sb(III) is easier to be sorbed to Fe and Mn oxyhydroxides and humic materials (Filella, M., Williams, P.A. et al., 2003). Sb mobilization in oxic environment is accompanied by the oxidation of Sb(III) to Sb(V) (Belzile, N., Chen, Y.W. et al., 2001).

Sediment with heterogeneous features along the depth is a reservoir for various Sb species including the soluble Sb species in porewater and complexes and minerals in the solid phase. It had been reported that release of Sb, As and Fe are related to redox condition variation along the depth, the shift from oxidic layer to anoxic layer cause a flux of Sb between solid phase and porewater (Dellwig, O., Leipe, T. et al., 2010). The equilibrium of Sb between solid and aqueous phase in sediment is also strongly affected by the adsorption capacities of metal oxyhydroxides (Arsic, M., Teasdale, P.R. et al., 2018). The diffusive gradient in thin films technique (DGT) has been used to investigate the bioavailability and mobility of metal(loid)s including Cu, Ni, Sb, and Zn in situ (Peng, Q., Wang, M. et al., 2017; Seah, K.C., Qasim, G.H. et al., 2017; Song, Z., Shan, B. et al., 2018). The DGT has been used to investigate Sb release from sediment at the millimeter scale to assess the mechanisms involved in Sb mobility (Jun, L., Hao, Z. et al., 2010; Ding, S., Xu, D. et al., 2016). Sb has been found to be released from sediment in wetlands and lakes around the world, but the factors involved in Sb mobilization need to be investigated further.

Here, we described the distribution and speciation of Sb in lake water and sediment. The aims of this work were (1) to identify features of Sb contaminants from textile and printing plants in shallow lake water and sediment. (2) to reveal Sb mobility in sediment rich in organic materials caused by urbanization and industrialization.

2. Materials and methods

2.1. Study area and sample collection

The study area was a 41.6 ha shallow lake located in the southeastern part of the Lake Taihu Basin (30°45′09"-30°45′45" N, 120°44′60" - 120°45′45"E), which has the densest plain river networks in China. Natural rivers and artificial canals surrounding and connecting to the study area transported nutrients and pollutants from Lake Taihu and local towns into the study area. The areas around Lake Taihu have been rapidly urbanized in the last 30 years, textile manufacturing and printing are the main industries. Two lake estuaries in the south and an outlet in the north connect the plain river network. The lake has an annual mean water storage capacity of 1.8×10^6 m^3, and daily water outflow/inflow is about 0.833×10^6 m^3. The water residence time was conducted as about

2.4 days. A survey on the local water quality indicated that the highest Sb concentration was 10 μg/L, very close to the World Health Organization drinking water safety threshold. Water samples were collected from 10 sites (W 1−10) and sediment from five sites (S 1−5). The site locations are shown in Fig. 1. Each water or sediment sample was stored at 5 °C until analysis.

2.2. DGT samplers deployment

DGT piston was a molded plastic cylinders (diameter 25 mm) containing, from bottom to top, a 0.4 mm binding resin gel, a 0.8-mm diffusive gel, and a 0.1-mm filter for water. DGT probe for sediment was a plastic rectangular (150 mm × 20 mm) covering the same three layers as DGT piston. The DGT pistons, DGT probes were all purchased from EasySenser®. Zirconium oxide based binding resin gels (ZrO-Chelex) were chosen for its reliable simultaneous measurement of multiple ions, including Cr(VI), Se(VI), Mo(VI), As(V), P(V), Sb(V), As(III), Cd(II), Co(II), Cu(II), Zn(II), Mn(II), Pb(II), Ni(II) and Fe(II) (Ding, S., Xu, D. et al., 2016). The 0.8-mm agarose diffusive gel was covered with a 0.1 mm-thick polyvinylidene fluoride filter, PVDF.

DGT probes and Peepers deployed in the sediment provided high spatial resolution in the vertical direction and measured the mean flux of labile species to the device during the deployment (Zhang, H., Davison, W. et al., 1995). The ZrO-Chelex binding gel can quickly bind Sb(V) and other ions like P(V), Fe(II), Mn(II), Pb(V), Ni(II) that are in the labile equilibrium upon perturbation by the probe (Ding, S., Xu, D. et al., 2016). Every 2 circular DGT pistons (20 in total) were deployed under about 12−13 cm from water surface and 2−3 m above the sediment. Every 2 DGT probes (10 in total) were placed vertically into 5 sediment samples collected within polyvinyl chloride, PVC tubes. The deployment time (t) for DGT pistons in water and DGT probes in sediment were 24 h. The Peeper was also a plastic rectangular (150 mm × 20 mm) but only covering with separated chamber to collect porewater. Each Peeper was tightly bounded to the back of DGT prob, and deployed in sediment simultaneously to collect porewater. DGT pistons and probes were deoxygenated through nitrogen purging in purified water in 24 h before deployment in the water and sediment.

The DGT labile concentration at the diffusion layer-sediment interface (C_{DGT}) was calculated using the equation:

$$C_{DGT} = \frac{M\Delta g}{DtA} \tag{1}$$

where M is the mass sorbed by the DGT, Δg is the thickness of the diffusive gel (0.8 mm), D is the diffusion ratio of the target species, A is the area of the binding gel, and t is the deployment time (24 h). M was determined by eluting Sb from the resin gel using 2 mL of 2 mol/L HNO$_3$. It was assumed that C_{DGT} remain relatively constant during the deployment because of the time to reach equilibrium between aqueous and solid phase are generally much less than deployment time (24 h).

The DIFS model proposed by (Harper, 2000) was used to describe the sediment to porewater desorption kinetics (k_{-1}) and porewater to sediment adsorption kinetics (k_1). The DIFS model was running upon the R, ratio of C_{DGT} to the labile Sb concentrations in porewater C (Equation (2)) and the K_d, distribution coefficient between the labile Sb contents in solid phases (C_s) and concentrations in the porewater (Equation (3)).
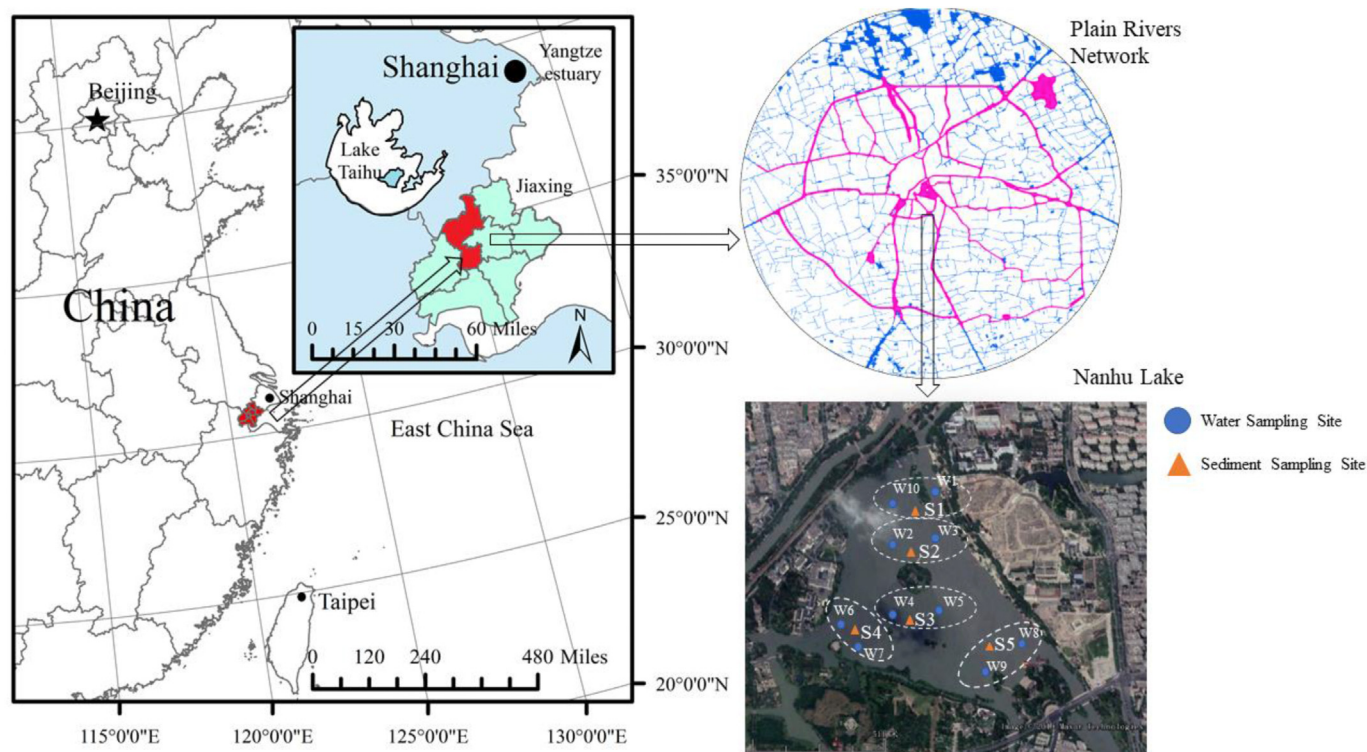
$$R = \frac{C_{DGT}}{C} \tag{2}$$

Fig. 1. Water and sediment sampling sites at the Lake Nanhu located in the plain rivers network of the Lake Taihu Basin.

$$K_d = \frac{C_s}{C} \tag{3}$$

The response time (Tc) was driven from DIFS model knowing R and K_d and was used to calculated k_1 and k_{-1} using the equation:

$$k_{-1} = \frac{1}{T_c(1 + K_d P_c)} \tag{4}$$

$$k_1 = k_{-1}K_d P_c \tag{5}$$

2.3. Water column analysis

The dissolved oxygen concentration (DO), oxidation-reduction potential (ORP), pH, temperature (TEMP), and the specified conductance (SPC) were measured in situ by using a YSI ProPlus system. The chemical oxygen demand (COD$_{Mn}$), nitrogen, ammonia and phosphorus concentrations were determined in the laboratory within 24 h of each sample being collected using previously published methods (Fishman, M.J., Erdmann, D.E. et al., 1983). Chlorophyll a (Chl.a) was collected by passing a water sample through a Whatman 0.45 μm mixed cellulose ester membrane (GE Healthcare Bio-Sciences, Pittsburgh, PA, USA) and determined by measuring the absorbance of an acetone extract of the dried membrane at 663 and 645 nm. The total organic carbon (TOC) was analyzed by TOC Analyzer (Shimadzu, Kyoto, JAPAN). An aliquot of each water sample was passed through a 0.45 μm membrane filter and the Sb species concentrations were determined by high-performance liquid chromatography-hydride generation-atomic fluorescence spectrometry (HPLC-HG-AFS) for Sb species in water. The Sb species were separated using a Thermo UltiMate 3000 high-performance

liquid chromatograph (Thermo Fisher Scientific, Waltham, MA, USA) and detected using a hydride-generation atomic fluorescence spectrometer (PSA Analytical, Orpington, UK). Separation was achieved using a Hamilton PRP-X100 column (100 mm long, 4.1 mm i.d.; Hamilton, Reno, NV, USA). A 5 mL water sample was passed through a 0.7 μm glass fiber filter to remove suspended solids (SS) before being analyzed. The Sb (III) standard solution of K(SbO)C$_4$H$_4$O$_6$H$_2$O (99.95% pure; Sigma-Aldrich, St Louis, MO, USA) was prepared. The Sb(V) standard solution was prepared by dissolving KSb(OH)$_6$ (99.95% pure; Sigma-Aldrich). It is difficult to quantify organoantimony accurately because of a shortage of commercial standards in China, but the mechanism of HPLC-HG-AFS made it possible to determine organoantimony relatively reliably. The chromatographic mobile phase was 20 mmol/L of ethylenediaminetetraacetic acid (EDTA) and 2 mmol/L potassium hydrogen phthalate powder (Aldrich, 99.99%) in water at pH 4.5. The second mobile phase, 50 mmol/L (NH$_4$)$_2$HPO$_4$ solution in water at pH 8.3, was used in a gradient program.

2.4. Sediment samples analysis

The top 0−20 cm of sediment samples and ~15 cm of the overlaying water were collected into polyvinyl chloride column, transported to the laboratory, and left to stand for 24 h. After the DGT probes and Peeper had been deployed and recovered, each sediment sample was divided into 2 cm deep segments, freeze-dried, and then ground. The sample was then passed through a 100-mesh nylon sieve and a 200-mesh nylon sieve to remove stones, dead organisms and coarse debris. The nitrogen content was determined using the standard Kjeldahl-method. The ignition loss (IG) of dried sediment (550 °C for 1 h) was used to reveal the organic matters in sediment.

Sequential extractions by using different chemical reagents is

the most common method for evaluating the features of metals in the sediment (Sahuquillo, A., López-Sánchez, J.F. et al., 1999; Gleyzes, C., Tellier, S. et al., 2002).The Common Bureau of Reference (BCR) sequential extraction procedure and Terrier method (Tessier, A., Campbell, P.G.C. et al., 1979) are the two widely used method, which have given good accuracy and reproducibility in many cases (Gleyzes, C., Tellier, S. et al., 2002). The BCR method, is a standard procedure defined in the European Water Framework Directive, can be used for a wide range of sediments to give readily comparable results. The Sb fractions in the sediment samples were determined by BCR-sequential extraction. A ~0.2 g aliquot of a treated sediment was subjected to the BCR sequential extraction procedure. The exchangeable fraction (F1) was extracted using 0.11 mol/L CH_3COOH, the reducible fraction (F2) was extracted using 0.5 mol/L $NH_2OH \cdot HCl$ and 2 mol/L HNO_3, the oxidizable fraction (F3) was extracted by 8.8 mol/L H_2O_2 and 1 mol/L NH_4CH_3COO, and the residual fraction (F4) was extracted using H_2O_2, and HCl. A ~0.2 g aliquot of sediment sample was digested by aqua regia to give the total contents of Sb. The total digested Sb were measured using an Agilent 7500a inductively coupled plasma mass spectrometer, ICP-MS (Agilent Technologies, Santa Clara, CA, USA).

2.5. Statistic and data analysis

Correlation tests were performed using SPSS 22 software (IBM, Armonk, NY, USA). Quality assurance and quality control were assessed by analyzing duplicates, method blanks and standard materials, GSB 04−1767 -2004 provided by National Nonferrous Metal and Electronic Materials Analysis and Testing Center, and CNS392 provided by Sigma-Aldrich. The limits of Sb determination (LODs) for methods coupled with HPLC-HG-AFS and ICP-MS are 0.1 μg/L, 0.02 μg/L separately. The results were considered reliable if the analysis error for repeat standard materials was ~5%, and the analytical precision for replicate samples was ≤10%. The recoveries of Sb analysis in water and sediment were all above 90%. The sums of all the sequential extraction fractions were 90%−105% of the Sb concentrations in the aqua regia digests.

3. Results and discussions

3.1. Antimony species in lake water

The results of the water analyses are shown in Table 1. The study area was a typical shallow lake with an oxidizing and alkaline water environment (pH 7.68 to 8.36, ORP 1.72−1.94 V). The mean levels of TOC, TN, NH_4^+ and TP in the water were 6.27, 5.15, 0.8 and 0.24 mg/L respectively, and the of Chl.a concentrations were 6.89−32.96 mg/

L, indicating that the lake was eutrophic. The aqueous phase contained antimonates, antimonites and organoantimony. The relative high levels of Sb species, COD_{Mn} and SS were mainly attributed to the pollution from the local towns and textile plants (Yao, C., Jiang, X. et al., 2019). The toxicities of Sb species increase in the order organoantimony < Sb(V) < Sb(III), but the abundances of the species in natural water decrease in the order Sb(V) > Sb(III) > organoantimony (Wilson, S.C., Lockwood, P.V. et al., 2010). Unlike in natural waters where prevalent species are dominant, in some sampling sites Sb in water was mainly trivalent that should be attributed to widespread use of antimony potassium tartrate in the textile plants.

The DGT labile Sb concentrations ($[Sb]$-C_{DGT}) in water were $0.42 − 3.80$ μg/L, and significantly correlated with the Sb(III) and Sb(V) in water (Person's r = −0.88 and 0.99, respectively, P < 0.05). $[Sb]$-C_{DGT} positively correlated with Sb(V) concentrations, which was attributed to selectively accumulation of Sb species by the binding agents (ZrO-Chelex). The measured species, e.g. SbO_3^-, $Sb(OH)_6^-$, and $Sb(OH)_5$, would have reached equilibrium with ZrO (Ding, S., Xu, D., et al., 2016), but the Sb(III) can rarely bind to ZrO (Ungureanu, G., Filote, C. et al., 2016; Ungureanu, G., Santos, S.C.R. et al., 2017). So, the DGT-labile Sb we determined would therefore mainly have been Sb(V) and could be treated as being mostly Sb(V).

The correlationship between the organoantimony and Chl.a (Pearson's r = 0.96, P < 0.05) had been witnessed in the study area. Methylation has been identified as mechanism of planktonic algae's resistance to toxicity of As (Levy, J.L., Stauber, J.L. et al., 2010). There is no strong evidence that methylation has also happened on Sb detoxicity in algal communities. It is possible that the planktonic algae absorb Sb species and transform them into organoantimony, then the decay of dead algae discharged organoantimony into the water. The methylations of As had been found in the uptake of phosphorate by planktonic (Granchinho, S.C.R., Cullen, W.R. et al., 2004). Whether Sb is absorbed and methylated by planktonic need further experimental confirmation in the future.

3.2. Antimony fractions in sediment

Sediment is a crucial lake ecosystem component because it can store the storage of nutrients and plays vital role in the collection and release of persistent toxic substances. The surficial sediment pH were ~7.5, temperature were ~7−9 °C, ORP ranged from −301 to 453 mV. The surficial sediment bioproduction index, determined by IG (4.7%−14%) and N-content (0.5−3.3 mg/g) of surficial sediment was 2.8. The lake was mesotrophic/eutrophic from sedimentological viewpoint, and there were some anoxic areas in the sediment

Table 1
The physichemical characteristics of water in situ and concentrations of Sb species in water samples.

	pH	ORP (v)	TEMP (°C)	SPC (μs/cm)	SS (mg/L)	TOC (mg/L)	TN (mg/L)	TP (mg/L)	NH_4^+ (mg/L)	Chl.a (mg/L)	Sb(V) (μg/L)	Sb(III) (μg/L)	Organo-antimony (μg/L)	$[Sb]$-C_{DGT} (μg/L)
W1	7.68	1.73	9.0	578	12.00	6.38	4.99	0.27	0.56	7.12	0.93	2.90	0.10	0.83
W2	8.35	1.80	9.1	563	9.50	6.44	5.40	0.22	0.82	6.89	0.48	5.88	<0.10.	0.42
W3	8.24	1.85	9.2	562	13.00	6.13	5.06	0.24	0.65	32.96	1.15	3.01	0.61	1.00
W4	8.30	1.81	7.3	562	14.00	6.32	5.70	0.19	0.80	23.32	3.50	1.12	0.32	3.80
W5	8.36	1.72	7.5	560	11.00	6.21	5.21	0.22	0.84	13.93	0.69	3.78	0.22	0.63
W6	8.23	1.75	7.9	560	13.00	6.45	5.06	0.22	0.80	15.79	3.15	1.56	0.25	3.08
W7	8.24	1.79	7.6	561	10.00	6.46	5.40	0.23	0.94	27.16	2.11	1.75	0.35	2.06
W8	8.21	1.73	9.1	560	12.00	6.48	5.01	0.23	0.93	8.27	1.05	3.67	0.16	0.93
W9	8.25	1.94	8.6	562	17.50	5.87	4.86	0.28	0.97	32.50	2.13	1.58	0.52	1.98
W10	8.17	1.74	9.3	564	18.00	5.95	4.81	0.27	0.72	16.78	2.06	1.63	0.24	1.87

ORP = oxidation−reduction potential, TEMP = temperature, SPC = specific conductance, SS = suspended solid concentration, TOC = total organic carbon concentration, TN = total nitrogen concentration, TP = total phosphorus concentration, NH_4^+ = ammonium concentration, Chl.a = chlorophyl a concentration, Sb(V) = Sb(V) concentration, Sb(III) = Sb(III) concentration, Organoantimony = organoantimony concentration, $[Sb]$-$CDGT$ = Sb concentration at the DGT diffusion layer−sediment interface.
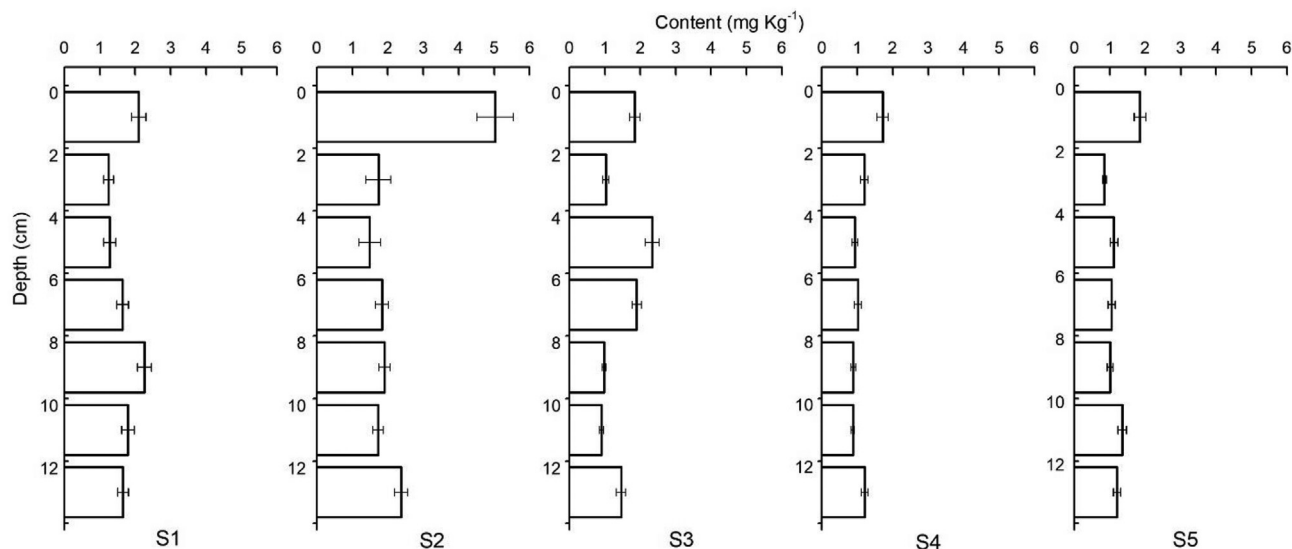
Fig. 2. The total Sb contents in S1, S2, S3, S4, S5 sediment samples.

surface. The Sb contents of the sediment were $0.82-4.70$ mg kg^{-1} and spatial distributions of Sb in lake sediment were as shown in Fig. 2. The Sb contents were higher in sediment from the central lake sites (S2 and S3) and sediment−water interface (SWI) $0-2$ cm deep than in the deeper sediment. The exchangeable fraction (F1) contained the most labile metal(loid)s in the sediment, such as Sb (III) oxyhydroxides and other poorly soluble antimony oxides. The reducible fraction (F2) contained Sb complexes with Fe/Mn oxides (Feyte, S., Tessier, A., Gobeil, C., Cossa, D., 2010). The oxidizable fraction (F3) contained Sb bounded to organic matters, sulfides. Sb of F2 and F3 could be transformed into more labile forms that are bioavailable to macrophytes and plants under reducing conditions (Olayinka, K.O., Oyeyiola, A.O. et al., 2011). The residual fraction (F4) contained Sb-bearing minerals formed in long-term mineralization, which are quite stable and rarely participate in environmental reactions. The percentages of F1 were much higher in sediment surface, the percentages of labile fraction (F1+F2) were decreased from the surface to deeper sediment, as shown in Fig. 3. The residual Sb contents increased from 0.29 mg kg^{-1}, 0.34 mg kg^{-1} in the lake estuaries (S4, S5), to 0.62 mg kg^{-1}, 0.94 mg kg^{-1} in the central areas (S2, S3) and 1.02 mg kg^{-1} in the lake outlet (S1). While lake central (S2, S3) had more the labile Sb contents, lake estuaries (S4, S5) owned the higher percentages of the labile Sb content. Sb in lake sediment is gradually forming into more stable Sb-bearing compounds.

3.3. Kinetics of Sb(V) release

The results of DIFS calculation indicated the kinetics of Sb release, as shown in Fig. 4. [Sb(V)]-C$_{DGT}$ can be categorized into 3 levels: (1) $1-2$ μg/L in the surficial sediment ($0-4$ cm deep) at S1 and $4-12$ cm deep at S2 and S3; (2) $3-4$ μg/L in sediment from S4 and S5; (3) the concentrations in specified area even much higher than initial concentrations of porewater before deployment C_o ($4-5$ μg/L). The R values (Table 2) indicated that the first level of Sb in sediment ($R < 0.95$) can resupply the porewater but insufficient to maintain. Sb in the second level ($R \geq 0.95$) was continuously transported to porewater during deployment of the DGT probes, but porewater concentrations were slightly lower than initial concentration before. Sb in the third level could resupply to porewater sustainably and the DGT concentrations even exceed the initial concentrations in the porewater. The Sb(III) concentrations in porewaters were $0-1$ μg/L and did not markedly vary with depth.

The kinetics parameters for Sb(V) release are shown in Table 2. The K_d values were $113-450$ cm^3/g and were higher for sustained cases than the partial sustained cases, indicating that a higher percentage of labile Sb in sediment increased the capacity of the sediment to sustainably resupply Sb to the porewater. For the partial sustained cases, the response time T_c were $9382-11731$ s, indicating that a longer time is required to reach equilibrium in the exchange between aqueous and solid phase under the
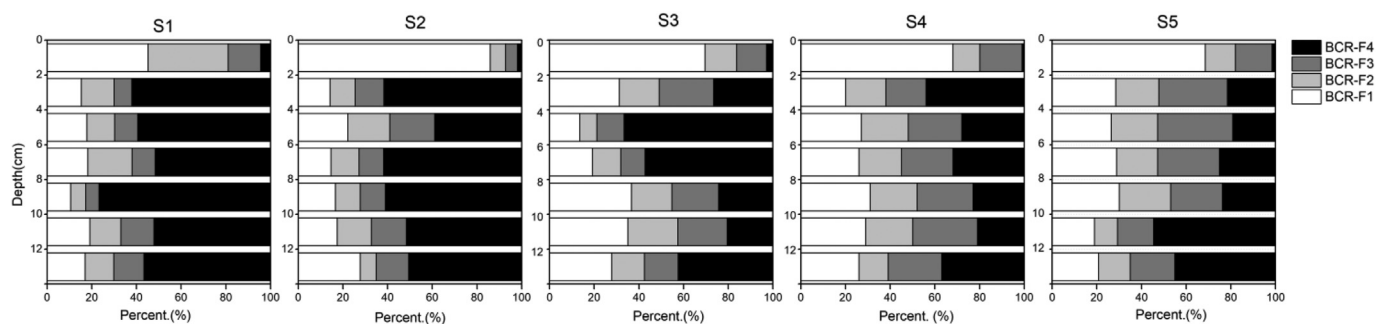

Fig. 3. The percentages of BCR sequential extraction fractions (the exchangeable fraction (F1) that contained soluble Sb oxides/oxyhydroxides, the reducible fraction (F2) that contained the Sb complexes with Fe/Mn oxides, the oxidizable fraction (F3) that contained the Sb bounded to organic matters, sulfides and the residual fraction (F4) that contained Sb-bearing minerals) in S1, S2, S3, S4, S5 sediment samples.
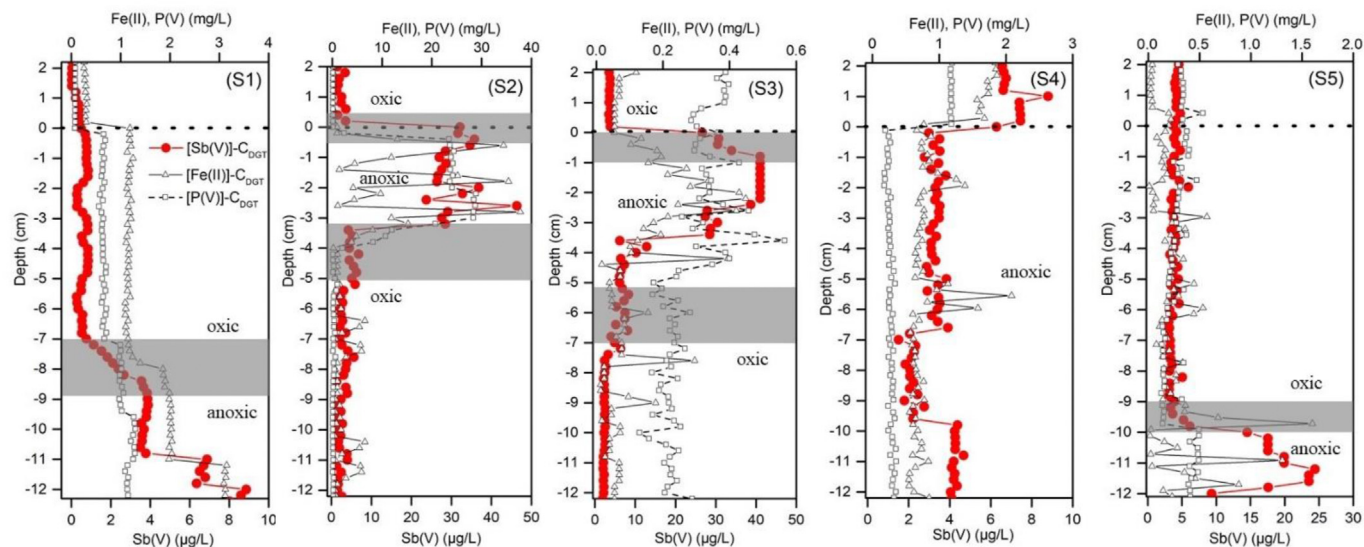
Fig. 4. Vertical distributions of the DGT labile Sb(V), P(V) and Fe(II) concentrations ([Sb(V)]-CDGT, [P(V)]-CDGT and Fe(II) -CDGT) in overlaying water and sediment from S1, S2, S3, S4 and S5. The dashed lines indicate the sediment-water interface. The gray areas represent the redox transitional zone.

Table 2
Kinetics parameters for Sb in sediments at different depths calculated using the DIFS model.

	Sediment Layer	R	K_d (cm^3/g)	T_c (s)	k_1 ($\times$ 10^{-4} s^{-1})	k_{-1} ($\times$ 10^{-7} s^{-1})
S1	Surficial	0.28	225	11731	0.84	12.4
	Middle	0.31	113	10445	0.93	27.4
	Deep	0.97	450	341	29.1	215
S2	Surficial	0.98	384	337	29.4	255
	Middle	0.33	270	9978	0.99	12.2
	Deep	0.34	250	9675	1.02	13.6
S3	Surficial	0.99	396	334	29.7	250
	Middle	0.96	280	343	28.8	343
	Deep	0.35	220	9382	1.05	15.9
S4	Surficial	0.98	250	378	29.4	392
	Middle	0.95	238	387	28.5	399
	Deep	0.96	375	344	28.8	256
S5	Surficial	0.95	330	347	28.5	288
	Middle	0.95	237	346	28.5	401
	Deep	0.98	350	337	29.4	280

perturbation. For the sustained cases, the response time T_c were 336−347 s significantly shorter than the partial sustained cases. indicating that equilibrium was reached more quickly. These results were supported by the adsorption constant k_1 that ranging from 28.5 $\times$ 10^{-4} s^{-1} to 29.4 $\times$ 10^{-4} s^{-1} and the desorption constant k_{-1} ranging from 215 $\times$ 10^{-7} s^{-1} to 401 $\times$ 10^{-7} s^{-1} for the sustained cases. The k_1 and k_{-1} values of the partial sustained cases were 0.84 $\times$ 10^{-4} to 1.05 $\times$ 10^{-4} s^{-1} and 12.4 $\times$ 10^{-7} to 27.4 $\times$ 10^{-7} s^{-1}, respectively. There were no significant differences between the kinetics parameters for the sustained and partial sustained cases, indicating that the mechanisms for both cases were same.

3.4. Simultaneous release of Fe(II), P(V) and Sb(V)

The DGT labile Sb(V), P(V) and Fe(II) concentrations ([Sb(V)]-CDGT, [P(V)]-CDGT and Fe(II) -CDGT) are displayed in Fig. 4. [Fe(II)]-CDGT, [P(V)]-CDGT, and [Sb(V)]-CDGT in S1 increased dramatically with depth from 7 cm deep and were highest in S2 and S3 at 0 − 4 cm deep and in S5 at 10 − 12 cm deep. [Fe(II)]-CDGT, [P(V)]-CDGT, and [Sb(V)]-CDGT remained relatively constant with depth. Sustainable release of Sb(V) was accompanied with simultaneous Fe(II), P (V) release from solid phase.

The Fe oxides, including hydroxides and oxyhydroxides, are very active sorbents in natural environmental (Cui, X.D., Wang, Y.J. et al., 2015). The Fe oxyhydroxides are the key factors affecting the P cycle in the shallow lake sediments and Fe−P fraction is the main labile P in lake sediment in the Taihu Basin (Yuan, H., Shen, J. et al., 2010). The formation of Fe-oxyhydroxophosphate (−FeO(OH)−PO4) through adsorption and co-precipitation is the main source of the Fe−P fraction in pelagic sediment in the Baltic Sea and Black Sea (Dellwig, O., Leipe, T. et al., 2010). Ferric hydroxides (Fe(OH)$_3$) and goethite (−Fe(O)OH) can steadily absorb Sb(III) over a wide pH range, and the adsorption mechanism is through surface complexes on hydroxide radical (Leuz, A., Moench, H. et al., 2006). The Sb was involved into Fe, P cycle as trace metalloid that [Fe(II)]-CDGT, [P(V)]-CDGT were 0.5 − 40 mg/L, [Sb(V)]-CDGT were 4 − 50 μg/L in sustained sediment reflux area. Fe oxides would have sorbed Sb at the oxic layer in the overlaying water and sediment where Fe−P complexes were formed by scavenging phosphate. Phosphate (PO$_4^{3-}$) and Fe^{2+} in sedimentary reflux were detected by DGT under anoxic condition (ORP: 366 to −344 mV). In the meanwhile, the antimonate was discharged from Fe−Sb complexes. Therefore, Fe-rich particles in the water and sediment would have settled labile trace metal(loid)s such as Sb from the aqueous phase to solid. But a

shift from oxic to anoxic environment condition would have these Sb in sediment been labile again.

3.5. Release of Sb in the anoxic layer

Simultaneous release of Fe(II), P(V) and Sb(V) only occurred in the specified areas as mentioned above, where redox conditions had steep gradients from areas without sustained labile metal(loid)s release. As shown in Fig. 4, the redox transitional zones were located in relatively deep (7 − 10 cm) sediment at S1 and S5, of which from overlaying water to transitional zones were oxic layer, below the transitional zones were anoxic layer. There was an entirely anoxic zone from the overlaying water to deep sediment at S4. At S2 and S3, the anoxic layers were between the surface and moderately deep sediment, and the oxic layers were below the moderately deep sediment (3 − 7 cm). Anoxic layers ordinarily occur in the dozens of meters deep in lake sediment and even hundreds of meters deep in sea sediment. However, the anoxic layers were relative shallow in the study area. The relatively high organic matter contents (IG 7.35%−13.00%) of surficial sediment at S2, S3, S4 may have caused the shallow anoxic layer at these sites (ORP -356 mV to −301 mV). Oxygen can eventually penetrate surface to ~10 cm deep and gradually change the redox condition, like at S1 and S5. However, organic matter (biota and urban and industrial pollutants) would have consumed all of the oxygen in sediment surface even though oxygen was continually supplied (as dissolved oxygen) by the water.

The redox condition played a vital role on the adsorption and desorption of Sb in the lake sediment. The linear regressions of ORP for sediment at different depths throughout the study area against the response time (T_c) and [Sb(V)]-C_{DGT} are shown in Fig. 5(a). The positive linear relationship between the ORP and $\log_{10}(T_c)$ that sediment aqueous-solid two phases system take longer time to reach equilibrium in the oxic layers (ORP >150 mV) indicated the release of Sb in the anoxic layers (ORP -366 to −344 mV) are faster. The $\log_{10}(T_c)$ values in the anoxic layers were similar, indicating that Sb was released through the same mechanism in all of the anoxic layers. [Sb(V)]-C_{DGT} had a better negative linear regression with the ORP for the oxic than anoxic layers, but [Sb(V)]-C_{DGT} in the anoxic layers were between 4−40 μg/L. The variation in [Sb(V)]-C_{DGT} were caused by different amounts of Sb being released at different sites during 24 h. Although there was no line regression of labile Sb contents (F1+F2) with $\log_{10}(T_c)$ or [Sb(V)]-C_{DGT} as shown in Fig. 5(b). The positive correlation between [Sb(V)]-C_{DGT} and labile Sb contents (F1+F2) (Pearson'r = 0.609, P > 0.1) indicated that more labile content in solid phase bring out higher rate of release. However, labile Sb content (F1+F2) had seldomly impact on kinetic parameter of DIFS (T_c), which is eventually responded to the sediment ORP. Therefore, the Sb released of Sb from sediment to porewater was controlled by the redox conditions, and the amount of Sb resupplied from sediment to the porewater was controlled by the labile Sb content of the sediment.

The pollutants through the fluvial transportation caused the spatial distribution of Sb and the anoxic layer in sediment surface. At the lake estuary S4, the anoxic layer extended from the over-laying water to deeper sediment. This phenomenon has been witnessed in other eutrophic or contaminated lakes and wetlands. Colloidal suspensions over the sediment surfaces would have consumed oxygen and formed the anoxic layers that dissolved oxygen could not penetrate. Then these pollutants would have spread throughout the lake and gradually precipitated on the sediment surface at the lake central S2, S3, where the oxygen could penetrate the anoxic layer to the deeper sediment. The anoxic layers in the sediment surface were dark color and contained considerable amounts of organic matters (IG 10% − 13%) because of
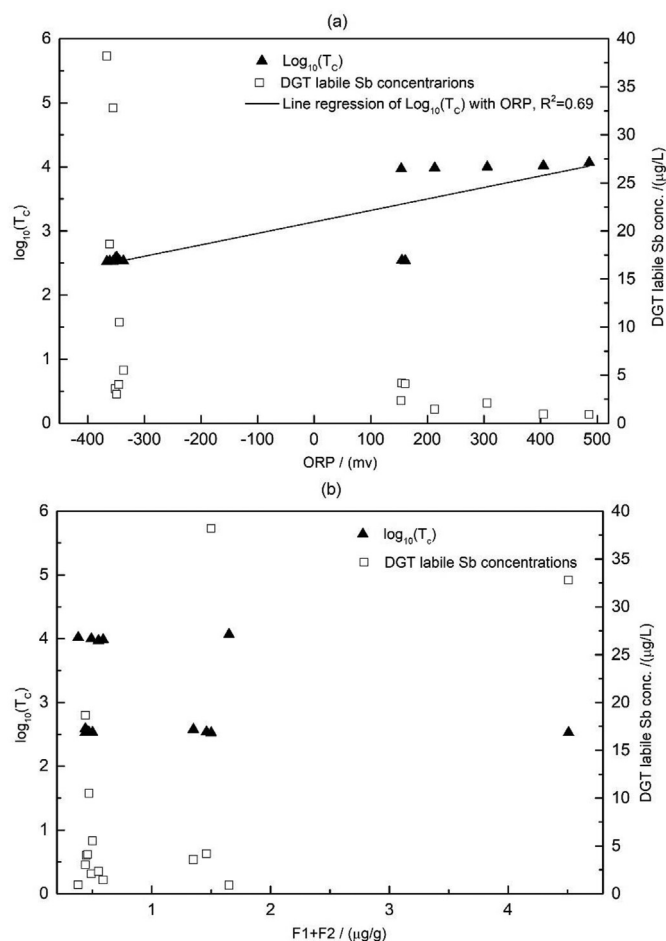

Fig. 5. Linear regressions of $\log_{10}(T_c)$ and the DGT labile Sb concentrations in sediment from different depths against (a) oxidation−reduction potential (ORP) and (b) the Sb concentration of the labile fractions F1+F2.

decaying algae, organic pollutants from local textile plants and local towns. Ordinary organic matters (e.g. humic and fulvic substances) in dark color sediment, reduced the mobility of Sb by preventing Sb(III) oxidation and sorption on a variety of functional groups (Pilarski, J., Waller, P. et al., 1995). Organic matters in the study area made sediment surface of S2, S3, S4 the anoxic layers and raised the mobility of Sb, which could be attributed to pollutants from textile plants and the sediment rich in ferric complexes.

Fe(II) is a good indicator of anoxic environment in sediment, and is commonly found in sediment in eutrophic lakes and anoxic pools (Ashcroft, S. J., Mortimer, C.,T., 1970). Fe(III) acts as an electron accepter in the bioreactions with Rhodoferax ferrireducens and in the reaction with reductants in anoxic sediment (Russell, Michael, J. et al., 2016). Simultaneous release of Fe(II), Sb(V) and P(V) indicates that electrons are transported from Fe(III) and P(III) when the Fe−Sb and Fe−P complexes are dissolved and discharged into porewater. Sb(III) is more stable than Sb(V) in its affinity for Fe and Mn oxides and organic matters (Wang, X., He, M. et al., 2011; Wang, X., He, M. et al., 2012). The relatively high Sb(III) concentrations in the water would lead to Sb(III) gradually forming complexes on solids and becoming mineralized in the oxic layers (ORP 154−486 mV). It has previously suggested that the formation of Fe−Sb secondary minerals (e.g. tripuhyite and schafarzikite) is one of the main geochemical processes in natural sediments and soils (Multani, R.S., Feldmann, T. et al., 2016). Future studies aimed at identifying the textural and geochemistry properties of Fe−Sb

complexes in sediment, particularly differences in oxic, anoxic, and transitional zones, should be performed.

4. Conclusions

The spatial distribution and environmental speciation of Sb in a shallow lake under the threat of textile industry were analyzed and Sb mobility in sediment was investigated by making DGT measurements. The field screening indicated that the textile industry brings out relatively high Sb(III), Sb(V) and organoantimony concentrations in the lake water. The continual Sb pollutants input through lake estuary have raised labile Sb content of the sediment surface, which are gradually forming into more stable Sb-bearing compounds in lake sediment.

Sb was seldomly mobile in the oxic sediment that can barely supply the porewater under perturbation of the DGT probes. While in the anoxic layers of overlaying water and sediment, the mobility of Sb was considerable that sustainable reflux from solid phase are maintained. The release of Sb from solid phase was decided by the redox condition, and the rate of release was controlled by the labile Sb content of the sediment.

Simultaneously release of Sb(V), Fe(II) and P (V) occurred in anoxic sediment during the DGT deployment. Sb(III) were sorbed on Fe(III) oxides and forming Fe–Sb complexes in the sediment. However, the anoxic environments (ORP -366 to -344 mV) due to pollutants rich in organic matters (IG 10% $-$ 13%) caused the dissolution of Fe–Sb, Fe–P complexes. Thus, the common assumption that Sb is relatively poorly mobile in sediment, particularly in the shallow lakes, may underestimated the potential mobilization of Sb in anoxic environment.

Statement

The manuscript represents valid work and that neither this manuscript nor one with substantially similar content under my authorship has been published or is being considered for publication elsewhere; and if requested we will provide the data or agree to allow the corresponding author to obtain and provide the data on which the manuscript is based examination by the editors. I state that all passages which have been taken out of publications of all means or unpublished material either whole or in part, in words or ideas, have been marked as quotations in the relevant passage. I also confirm that the quotes included show the extent of the original quotes.

Author contribution

Cheng Yao: Conceptualization, Methodology, Formal analysis, Investigation, Resources, Data curation, Writing – original draft, Writing – review & editing, Visualization; Feifei Che: Conceptualization, Methodology, Formal analysis, Writing – review & editing; Xia Jiang: Conceptualization, Writing – original draft, Writing – review & editing, Supervision, Project administration; Zhihao Wu: Methodology, Formal analysis, Writing – review & editing, Visualization; Junyi Chen: Investigation, Resources; Kun Wang: Investigation, Resources

Declaration of competing interest

The authors declare that they have no known competing financial interests or personal relationships that could have appeared to influence the work reported in this paper.

References

Arsic, M., Teasdale, P.R., Welsh, D.T., Johnston, S.G., Burton, E.D., Hockmann, K., Bennett, W.W., 2018. Diffusive gradients in thin films (DGT) reveals antimony and arsenic mobility differs in a contaminated wetland sediment during an oxic-anoxic transition. Environ. Sci. Technol. 52 (3) acs.est.7b03882.

Ashcroft, S.J., Mortimer, C.T., 1970. Thermochemistry of Transition Metal Complexes. Academic Press.

Belzile, N., Chen, Y.W., Wang, Z., 2001. Oxidation of antimony (III) by amorphous iron and manganese oxyhydroxides. Chem. Geol. 174 (4), 379–387.

Cui, X.D., Wang, Y.J., Hockrnann, K., Zhou, D.M., 2015. Effect of iron plaque on antimony uptake by rice (Oryza sativa L.). Environ. Pollut. 204 (SEP.), 133–140.

Dellwig, O., Leipe, T., M Rz, C., Glockzin, M., Pollehne, F., Schnetger, B., Yakushev, E.V., B Ttcher, M.E., Brumsack, H.J., 2010. A new particulate Mn–Fe–P-shuttle at the redoxcline of anoxic basins. Geochem. Cosmochim. Acta 74 (24), 0-7115.

Ding, S., Xu, D., Wang, Y., Wang, Y., Li, Y., Gong, M., Zhang, C., 2016. Simultaneous measurements of eight oxyanions using high-capacity diffusive gradients in thin films (Zr-oxide DGT) with a high-efficiency elution procedure. Environ. Sci. Technol. 50 (14), 7572.

Feyte, S., Tessier, A., Gobeil, C., Cossa, D., 2010. In situ adsorption of mercury, methylmercury and other elements by iron oxyhydroxides and organic matter in lake sediments. Appl. Geochem. 25 (7), 984–995.

Filella, M., Williams, P.A., Belzile, N., 2003. Antimony in the environment: a review focused on natural waters. Part 2. Relevant solution chemistry. ChemInform 34 (23), 125–176.

Fishman, M.J., Erdmann, D.E., Garbarino, J.R., 1983. Water analysis. Anal. Chem. 55 (5), 102–133.

Gleyzes, C., Tellier, S., Astruc, M., 2002. Fractionation studies of trace elements in contaminated soils and sediments: a review of sequential extraction procedures. Trends Anal. Chem. 21 (6), 451–467.

Granchinho, S.C.R., Cullen, W.R., Polishchuk, E., Reimer, K.J., 2004. The Effect of Phosphate on the Bioaccumulation and Biotransformation of arsenic(V) by the Marine Alga Fucus Gardneri. Springer Berlin Heidelberg.

Hu, X., He, M., Li, S., Guo, X., 2017. The leaching characteristics and changes in the leached layer of antimony-bearing ores from China. J. Geochem. Explor. 176, 76–84.

Jun, L., Hao, Z., Jakob, S., William, D., 2010. Performance characteristics of diffusive gradients in thin films equipped with a binding gel layer containing precipitated ferrihydrite for measuring arsenic(V), selenium(VI), vanadium(V), and antimony(V). Anal. Chem. 82 (21), 8903.

Leuz, A., Moench, H., Johnson, C.A., 2006. Sorption of Sb(III) and Sb(V) to goethite:? Influence on Sb(III) oxidation and mobilization. Environ. Sci. Technol. 40 (23), 7277–7282.

Levy, J.L., Stauber, J.L., Adams, M.S., Maher, W.A., Kirby, J.K., Jolley, D.F., 2010. Toxicity, biotransformation, and mode of action of arsenic in two freshwater microalgae (Chlorella sp. and Monoraphidium arcuatum). Environ. Toxicol. Chem. 24 (10), 2630–2639.

Multani, R.S., Feldmann, T., Demopoulos, G.P., 2016. Antimony in the metallurgical industry: a review of its chemistry and environmental stabilization options. Hydrometallurgy 164, 141–153.

Multani, R.S., Feldmann, T., Demopoulos, G.P., 2017. Removal of antimony from concentrated solutions with focus on tripuhyite (FeSbO4) synthesis, characterization and stability. Hydrometallurgy 169, 263–274.

Olayinka, K.O., Oyeyiola, A.O., Odujebe, F.O., Oboh, B., 2011. Uptake of potentially toxic metals by vegetable plants grown on contaminated soil and their potential bioavailability using sequential extraction. J. Soil Sci. Environ. Manag. 2, 220–227.

Peng, Q., Wang, M., Cui, Z., Huang, J., Chen, C., Guo, L., Liang, D., 2017. Assessment of bioavailability of selenium in different plant-soil systems by diffusive gradients in thin-films (DGT). Environ. Pollut. 225, 637–643.

Pierart, A., Shahid, M., Séjalon-Delmas, N., Dumat, C., 2015. Antimony bioavailability: knowledge and research perspectives for sustainable agricultures. J. Hazard Mater. 289, 219.

Pilarski, J., Waller, P., Pickering, W., 1995. Sorption of Antimony species by humic-acid. Water Air Soil Pollut. 84 (1), 51–59.

Russell, Michael J., Takai, Ken, Shibuya, Takazo, 2016. Free energy distribution and hydrothermal mineral precipitation in Hadean submarine alkaline vent systems: importance of iron redox reactions under anoxic conditions. Geochimica Et Cosmochimica Acta Journal of the Geochemical Society & the Meteoritical Society.

Sahuquillo, A., López-Sánchez, J.F., Rubio, R., Rauret, G., Thomas, R.P., Davidson, C.M., Ure, A.M., 1999. Use of a certified reference material for extractable trace metals to assess sources of uncertainty in the BCR three-stage sequential extraction procedure. Anal. Chim. Acta 382 (3), 317–327.

Seah, K.C., Qasim, G.H., Hong, Y.S., Kim, E., Kim, K.T., Han, S., 2017. Assessment of colloidal copper speciation in the Mekong River Delta using diffusive gradients in thin film techniques. Estuar. Coast Shelf Sci. 188, 109–115.

Song, Z., Shan, B., Tang, W., 2018. Evaluating the diffusive gradients in thin films technique for the prediction of metal bioaccumulation in plants grown in river sediments. J. Hazard Mater. 344, 360–368.

Tessier, A., Campbell, P.G.C., Bisson, M., 1979. Sequential extraction procedure for the speciation of particulate trace metals. Anal. Chem. 51 (7), 844–851.

Ungureanu, G., Santos, S., Rui, B., Botelho, C., 2015. Arsenic and antimony in water and wastewater: overview of removal techniques with special reference to latest advances in adsorption. J. Environ. Manag. 151, 326–342.

Ungureanu, G., Filote, C., Santos, S.C.R., Boaventura, R.A.R., Volf, I., Botelho, C.M.S., 2016. Antimony oxyanions uptake by green marine macroalgae. Journal of Environmental Chemical Engineering 4 (3), 3441–3450.

Ungureanu, G., Santos, S.C.R., Volf, I., Boaventura, R.A.R., Botelho, C.M.S., 2017. Biosorption of antimony oxyanions by brown seaweeds: batch and column studies. Journal of Environmental Chemical Engineering 5 (4), 3463–3471.

Wang, X., He, M., Xi, J., Lu, X., 2011. Antimony distribution and mobility in rivers around the world's largest antimony mine of Xikuangshan, Hunan Province, China. Microchem. J. 97 (1), 4–11.

Wang, X., He, M., Lin, C., Gao, Y., Lei, Z., 2012. Antimony(III) oxidation and antimony(V) adsorption reactions on synthetic manganite. Chemie der Erde - Geochemistry - Interdisciplinary Journal for Chemical Problems of the Geosciences and Geoecology 72 (4), 41–47.

Warnken, J., Ohlsson, R., Welsh, D.T., Teasdale, P.R., Chelsky, A., Bennett, W.W., 2017. Antimony and arsenic exhibit contrasting spatial distributions in the sediment and vegetation of a contaminated wetland. Chemosphere 180, 388–395.

Wilson, S.C., Lockwood, P.V., Ashley, P.M., Tighe, M., 2010. The chemistry and behaviour of antimony in the soil environment with comparisons to arsenic: a critical review. Environ. Pollut. 158 (5), 1169–1181.

Yao, C., Jiang, X., Che, F., Wang, K., Zhao, L., 2019. Antimony speciation and potential ecological risk of metal(loid)s in plain wetlands in the lower Yangtze River valley, China. Chemosphere 218, 1114–1121.

Yuan, H., Shen, J., Liu, E., Wang, J., Meng, X., 2010. [Space distribution characteristics and diversity analysis of phosphorus from overlying water and surface sediments in Taihu Lake]. Environ. Sci. J. Integr. Environ. Res. 31 (4), 954–960.

Zhang, H., Davison, W., Miller, S., Tych, W., 1995. In-situ high resolution fluxes of Cd, Cu, Fe, and Mn and concentrations of Zn and Cd in pore water by DGT. Geochem. Cosmochim. Acta 59, 418–419.

Zotov, A.V., Shikina, N.D., Akinfiev, N.N., 2003. Thermodynamic properties of the Sb(III) hydroxide complex Sb(OH)3(aq) at hydrothermal conditions. Geochem. Cosmochim. Acta 67 (10), 1821–1836.